FULL PAPER *Surgery*

Comparison of Mesenchymal Stem Cells Derived from Fat, Bone Marrow, Wharton's Jelly, and Umbilical Cord Blood for Treating Spinal Cord Injuries in Dogs

Hak-Hyun RYU[1)], Byung-Jae KANG[1)], Sung-Su PARK[1)], Yongsun KIM[1)], Gyu-Jin SUNG[1)], Heung-Myong WOO[2)#], Wan Hee KIM[1)] and Oh-Kyeong KWEON[1)*#]

[1)]*Department of Veterinary Surgery, College of Veterinary Medicine, Seoul National University, Daehak-dong, Gwanak-gu, Seoul 151–742, Korea*
[2)]*College of Veterinary Medicine and KNU Stem Cell Institute, Kangwon National University, Chuncheon 200–701, Korea*

(Received 13 February 2012/Accepted 26 July 2012/Published online in J-STAGE 9 August 2012)

ABSTRACT. Previous animal studies have shown that transplantation of mesenchymal stem cells (MSCs) into spinal cord lesions enhances axonal regeneration and promotes functional recovery. We isolated the MSCs derived from fat, bone marrow, Wharton's jelly and umbilical cord blood (UCB) positive for MSC markers and negative for hematopoietic cell markers. Their effects on the regeneration of injured canine spinal cords were compared. Spinal cord injury was induced by balloon catheter compression. Dogs with injured spinal cords were treated with only matrigel or matrigel mixed with each type of MSCs. Olby and modified Tarlov scores, immunohistochemistry, ELISA and Western blot analysis were used to evaluate the therapeutic effects. The different MSC groups showed significant improvements in locomotion at 8 weeks after transplantation ($P<0.05$). This recovery was accompanied by increased numbers of surviving neuron and neurofilament-positive fibers in the lesion site. Compared to the control, the lesion sizes were smaller, and fewer microglia and reactive astrocytes were found in the spinal cord epicenter of all MSC groups. Although there were no significant differences in functional recovery among the MSCs groups, UCB-derived MSCs (UCSCs) induced more nerve regeneration and anti-inflammation activity ($P<0.05$). Transplanted MSCs survived for 8 weeks and reduced IL-6 and COX-2 levels, which may have promoted neuronal regeneration in the spinal cord. Our data suggest that transplantation of MSCs promotes functional recovery after SCI. Furthermore, application of UCSCs led to more nerve regeneration, neuroprotection and less inflammation compared to other MSCs.

KEY WORD: canine, mesenchymal stem cell, spinal cord injury, transplantation.

doi: 10.1292/jvms.12-0065; *J. Vet. Med. Sci.* 74(12): 1617–1630, 2012

Following spinal cord injury (SCI), macrophage and microglial infiltration induces progressive tissue cavitation or glial cyst formation [11]. Reactive astrogliosis results in a glial scar that contains a deposition of dense collagenous extracellular matrix which inhibits axonal and cellular migration [44]. The endogenous capacity of the spinal cord to repair itself and regenerate is thought to be limited after SCI [12, 53]. Therefore, therapeutic strategies that involve exogenous cell replacement should be considered. Stem cell transplantation has recently been identified as a potential therapeutic modality for treating SCI [1, 2]. Adult mesenchymal stem cells (MSCs) exert neuroprotective effects through putative mechanisms including secretion of nerve regeneration factors and transdifferentiation [8]. Treatment of SCI using MSCs derived from adipose tissue [19, 36], bone marrow (BM) [38], Wharton's jelly (WJ) [52] and umbilical cord blood (UCB) [8] has been studied. Characterization [50] and neural differentiation capacities [41] of various MSCs have been investigated using FACS and differentiation test *in vitro*, respectively. However, *in vivo* studies comparing the effects of MSCs on nerve regeneration and functional recovery according to the origin of the cells have not been performed.

In this study, we transplanted MSCs derived from adipose tissue, BM, WJ and UCB mixed with matrigel into dogs with SCI. The purpose of this study was to (1) examine whether the transplanted MSCs can promote functional recovery of the hind-limbs and prevent inflammation and glial scarring, (2) identify which MSCs are more effective for neuro-protection and -regeneration, and (3) determine whether matrigel may act as a cellular bridge at the injury site.

MATERIALS AND METHODS

MSC isolation and culturing: Canine MSCs were obtained from gluteal subcutaneous fat, BM aspirates, WJ and UCB. The procedures were used based on protocols previously described [36, 40].

Adipose tissue was aseptically collected from subcutaneous fat in the hip of a 2-year-old dog under anesthesia. Fat tissues were washed extensively with PBS (Gibco, Billings, MT, U.S.A.), minced and digested with 1 mg/m*l* collagenase type I (Invitrogen, Carlsbad, CA, U.S.A.) at 37°C for 1 hr with intermittent shaking. The digested tissue was filtered through 100 μm nylon mesh and centrifuged at 200 g for 10 min. Pellet cells including stem cells were resuspended with Dulbecco's modified Eagle medium (DMEM; Gibco) supplemented with 10% fetal bovine serum (FBS; Gibco).

*CORRESPONDENCE TO: KWEON, O.-K., Department of Veterinary Surgery, College of Veterinary Medicine, Seoul National University, Daehak-dong, Gwanak-gu, Seoul 151–742, Korea.
e-mail: ohkweon@snu.ac.kr
# Equal contribution.

Resuspended cells were plated in T75 flasks and incubated overnight at 37°C with 5% humidified CO_2. Unattached cells were removed after 24 hr by washing with PBS, and the medium was replaced every 48 hr until the cells became confluent. When cells were >90% confluent, they were banked with banking solution (DMEM supplemented with 10% DMSO and 20% FBS) or subcultured.

BM was aseptically collected in heparinized tubes from the humeral bone of a 2-year-old dog under anesthesia. The marrow was diluted 1:1 with PBS. A Ficoll-Paque Plus (Amersham Biosciences, Uppsala, Sweden) density gradient was used to collect the buffy coat layer. The diluted marrow was gently placed on Ficoll-Paque solution and centrifuged at 400 *g* for 20 min. The isolated marrow stromal cells were washed with PBS and centrifuged at 200 *g* for 10 min.

Fresh canine umbilical cords were obtained from dogs that underwent a Cesarean section and stored in Hanks' balanced salt solution (HBSS; Gibco) at 4°C. Following disinfection in 70% ethanol for 30 sec, the umbilical cord vessels were removed while still in HBSS. The mesenchymal tissue in WJ was then minced into pieces of about 20 mm^3 in size and centrifuged at 200 *g* for 5 min. After the supernatant was removed by aspiration, the precipitate was treated with collagenase type I (1 mg/m*l*) at 37°C for 12 hr, washed and further digested with 2.5% trypsin (Gibco) at 37°C for 30 min. FBS was then added to the mesenchymal tissue to halt trypsinization.

Low-density mononuclear cells were isolated from UCB using a Ficoll-Plaque Plus density gradient. The diluted UCB was gently placed on Ficoll-Paque solution and centrifuged at 400 *g* for 20 min. Cells were then washed with PBS and centrifuged at 200 *g* for 10 min.

Pellet cells collected from BM, WJ and UCB were incubated in media for 24 hr and unattached cells were removed and cultured as described in adipose tissue.

Flow cytometry analysis: The cells were stained with fluorescein isothiocyanate (FITC)-conjugated antibodies against CD14 (clone CAM36A; VMRD, Pullman, WA, U.S.A.), CD34 (clone 1H6; Serotec, Kidlington, U.K.), CD45 (clone CADO18A; VMRD) and CD105 (clone SN6; Serotec). The cells were also stained with phycoerythrin (PE)-conjugated antibodies against CD44 (clone IM7; Abcam, Cambridge, U.K.), CD73 (clone 7G2; Abcam) and CD90 (clone DH2A; VMRD). Expression of the corresponding cell surface markers was measured by FACS Calibur (Becton, Dickinson and Co., Franklin Lakes, NJ, U.S.A.) using CELL Quest Pro (Becton, Dickinson and Co.) software.

Osteogenic differentiation: MSCs were cultured in osteogenic medium composed of low-glucose DMEM supplemented with 10% FBS, 10 mM β-glycerophosphate (Sigma-Aldrich, St. Louis, MO, U.S.A.), 0.1 μM dexamethasone (Sigma-Aldrich) and 50 μM ascorbic acid-2-phosphate (Sigma-Aldrich) for 14 days. Osteogenic differentiation was evaluated by calcium mineralization. Alizarin red S was used to determine the presence of calcium [32].

Adipogenic differentiation: MSCs were cultured in low-glucose DMEM supplemented with 10% FBS and when cells were >80% confluent, then switched to adipogenic medium [DMEM low-glucose medium with 10% FBS, 10 μg/m*l* insulin (Sigma-Aldrich), 1 μM dexamethasone (Sigma-Aldrich), 0.2 mM indomethacin (Sigma-Aldrich) and 0.5 mM isobutyl-methylxanthine (Sigma-Aldrich)] for 3 days. The cells were then grown in DMEM low-glucose medium with 10% FBS and 10 μg/m*l* insulin (Sigma-Aldrich) for 4 days. This procedure repeated twice for 14 days based on previous study [36]. The accumulation of neutral lipids was detected by staining the MSCs in a solution containing 0.5% Oil red O.

Neuronal differentiation: To induce neuronal differentiation, we exposed MSCs to a cocktail of induction agents as previously described [37]. To initiate neuronal differentiation, cells were washed with PBS and neuronal induction medium (NIM) consisting of serum-free DMEM with butylated hydroxyanisole (BHA; 200 μM), KCl (5 mM), valproic acid (2 mM), forskolin (10 μM), hydrocortisone (1 μM) and insulin (5 μg/m*l*). All MSCs were cultured for 3 days in NIM. Neuronal differentiation was assessed by neuronal morphology, and the expression of glia-, neuron- and oligodendrocyte-specific markers was also analyzed. The cells were stained with antibodies specific for glial fibrillary acidic protein (sc-6170; GFAP, 1:200; Santa Cruz Biotechnology, Santa Cruz, CA, U.S.A.), galactosylceramidase (sc-67352; GALC, 1:200; Santa Cruz Biotechnology), neuronal nuclear antigen (ab77315; NeuN, 1:200; Abcam) and neurofilament 160 (N5364; NF160, 1:200; Sigma-Aldrich). The cells were then stained with secondary anti-mouse Fluor 594 and anti-rabbit Fluor 594 (Invitrogen) antibodies. The cells were also stained with DAPI (Sigma-Aldrich) to visualize the nuclei.

Animals: Twenty healthy adult beagle dogs (7.6 ± 1.2 kg, male) were used. All of the dogs were judged to be in good health and neurologically normal. This study was approved by the Institute of Laboratory Animal Resources, Seoul National University, South Korea (SNU-100317). All dogs were cared for in accordance with the Animal Care and Use Guidelines of the Institute of Laboratory Animal Resources, Seoul National University, South Korea. The dogs were randomly assigned to five groups based on treatment at 7 days after SCI: (1) the control group that received injections of matrigel only in the lesion site (n=4); (2) the ADSCs group that received adipose tissue-derived MSCs mixed with matrigel (n=4); (3) the BMSCs group that received BM-derived MSCs mixed with matrigel (n=4); (4) the WJSCs group treated with WJ-derived MSCs mixed with matrigel (n=4); and (5) the UCSCs group that received UCB-derived MSCs mixed with matrigel (n=4). Spinal cords were harvested at 8 weeks after MSCs transplantation.

Preparation of matrigel: Matrigel was prepared from an unfractionated high-salt/urea extract of an Engelbreth-Holm-Swarm (EHS) tumor as previously described [14, 20] and stored at −20°C. Growth factor-depleted matrigel was obtained by precipitation with 20% ammonium sulfate as previously described [47]. Before use, the matrigel was thawed and maintained at 4°C until the MSCs were added.

Induction of SCI: The experimental dogs were placed under general anesthesia, and their spinal cords were then compressed by balloon compression as previously described

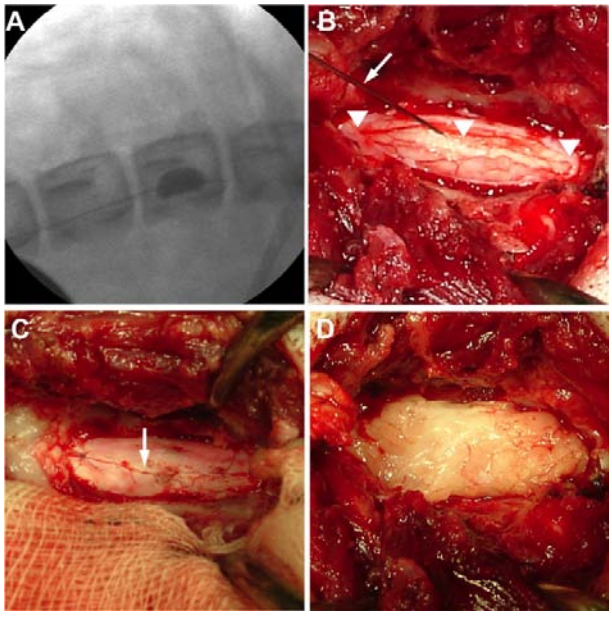

Fig. 1. Induction of canine spinal cord injury and transplantation of MSCs. (A) A 4-French embolectomy catheter was inserted into the epidural space through a left hemilaminectomy hole made in the L4 vertebral arch. The balloons were inflated with a contrast agent at the L1 level. (B) MSCs were transplanted using a Hamilton syringe (arrow) at three sites (cranial, epicenter and caudal; arrowhead) following dorsal laminectomy and durotomy at L1. (C) Dura was closed by a simple continuous 8-0 vicryl suture. (D) The laminectomy site was covered with thick layer of subcutaneous fat.

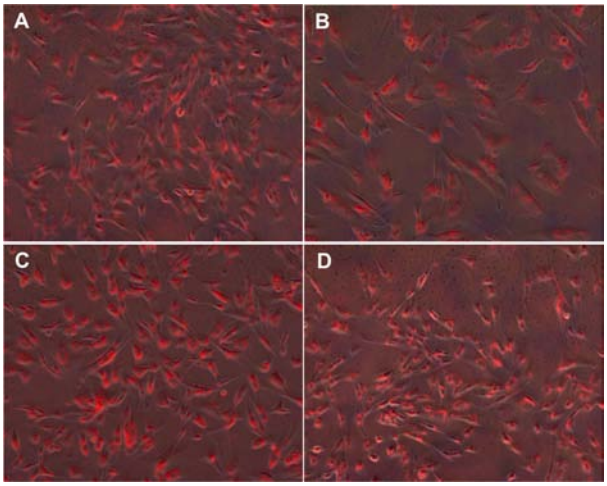

Fig. 2. Merged fluorescence and light-field images of labeled MSCs. MSCs were labeled with NEO-STEM^{TM} (TMSR50, red fluorescent nanoparticles) before transplantation. (A) Adipose tissue-derived MSCs, (B) Bone marrow-derived MSCs, (C) Wharton's jelly-derived MSCs, and (D) Umbilical cord blood-derived MSCs.

[36]. Dogs were anesthetized with intravenous administration (4 mg/kg) of tramadol (Toranzin; Samsung Pharm, Ind. Co., Ltd., Seoul, South Korea) and 6 mg/kg propofol (Anepol; Ha Na Pharm Co., Ltd., Seoul, South Korea) with 0.04 mg/kg atropine sulfate (Atropine; Je Il Pharmaceutical Co., Ltd., Seoul, South Korea) administered subcutaneously. Anesthesia was maintained by inhalation of 2% isoflurane (Aerrane; Baxter, Mississauga, ON, Canada). Datex-Ohmeda anesthesia monitor (Microvtec Display; GE Healthcare, Bradford, U.K.) was used to monitoring of physiologic measurements including rectal temperature, oxygen saturation, end tidal CO_2, electrocardiogram, minimum alveolar concentration, and pulse rate.

The hemilaminectomy was performed using a left paramedian approach at the fourth lumbar segment (L4). A 3.5-mm hole was made in the left vertebral arch at the L4 level using a high-speed pneumatic burr. A 4-French embolectomy catheter (Sorin Biomedica, Saluggia, Italy) was inserted into the hole made at the L4 vertebral arch. The balloon was advanced under fluoroscopic guidance until balloon of the catheter reached the first lumbar segment (L1) vertebral body. The balloon was then inflated with a 50:50 solution of contrast agent (Omnipaque; Amersham Health, Cork, Ireland) and saline at a dose of 40 μl/kg body weight (Fig. 1A). After 12 hr, the balloon was deflated and removed. All dogs were administered analgesics at a continuous infusion rate for 18 hr after skin closure. Post-operative analgesics contained morphine (Hwang Morphine; Ha Na Pharm) at 0.15 mg/kg/hr, lidocaine HCl (Lidocaine Injection 0.5% Yuhan; Yuhan Co, Ltd., Seoul, Korea) at 2 mg/kg/hr and ketamine HCl (Ketamine Injection 50 Yuhan; Yuhan Co, Ltd.) at 0.3 mg/kg/hr [36]. After the operation, the dogs were bandaged, monitored in an intensive care unit, and the degree of pain was assessed at 30 min intervals. Dogs that exhibited overt signs of discomfort were given IV infusions of tramadol (4 mg/kg). Suture materials were removed after 10 days. If needed, manual bladder expression was performed at least three times daily until voluntary urination was observed. The general condition and neurological status of the dogs were evaluated twice daily during the study. No complications were observed except for mild cystitis and muscle atrophy of the hind limbs. Two dogs developed a seroma at the surgical site that spontaneously resolved after 2 weeks.

Transplantation of MSCs: Transplantation of matrigel and MSCs was performed at 1 week after SCI in each group of dogs. The dogs were anesthetized as same methods as mentioned above. Dorsal laminectomy and durotomy were then performed at the first lumbar vertebra. Cells (1×10^5 cells/μl) suspended in 60 μl of matrigel were injected with a Hamilton syringe into dogs in each MSC group at three sites (cranial, epicenter, and caudal lesions; 20 μl/site) of the spinal cord parenchyma. This was followed by a 2 min delay before the needle was withdrawn (Fig. 1B). Thus, a total of 6.0×10^6 cells were grafted into each injured spinal cord. Only matrigel (60 μl) was injected into the control dogs at the three sites in the spinal cord parenchyma. Prior to injection, all MSCs were labeled with NEO-STEM^{TM} (TMSR50; red fluorescent nanoparticles, Biterials Co., Ltd., Seoul, South Korea) in order to facilitate identification of the cells within the histological specimens (Fig. 2A–D). Dura was closed by a simple continuous 8–0 vicryl suture (Fig. 1C). The lami-

Table 1. Comparison of the Olby score and Revised Modified Talov scale

Olby score			Revised Modified Tarlov scale	
No pelvic limb movement	no deep pain sensation	0	1	Flaccid hind limbs
	with deep pain sensation	1		
	but voluntary tail movement	2		
Non-weight-bearing protraction of pelvic limb with more than one joint involved	minimal movement (just one joint)	3	2	Tone in hind limb
	less than 50% of the time	4	3	Purposeful hind limb motion
	more than 50% of the time	5		
Weight-bearing protraction of pelvic limb	less than 10% of the time	6	4	Stands with assistance
	10–50% of the time	7		
	more than 50% of the time	8		
Weight-bearing protraction 100% of the time with reduced strength of pelvic limb	mistake > 90% of the time	9	5	Stands unassisted
	mistake 50–90% of the time	10	6	Limited ambulation
	mistake < 50% of the time	11		
Ataxic pelvic limb gait with normal strength	but mistakes made > 50% of time	12	7	Full ambulation
	but mistakes made < 50% of time	13	8	Climbs a 20° incline ramp half-way
Normal pelvic limb gait		14	9	Climbs 20° incline ramp

nectomy site was covered with a thick layer of subcutaneous fat (Fig. 1D). The incision was closed routinely.

Histopathological and immunofluorescence assessments: The dogs were euthanized at 8 weeks after MSC transplantation. The spinal cords from the 12th thoracic segment to the third lumbar segment of all dogs were removed. The spinal cords were placed in 10% sucrose for 12 hr and subsequently immersed in a 20% sucrose solution overnight at 4°C. Dura was removed by scissors, embedded in optimal cutting temperature compound (Tissue-Tek® O.C.T compound, Sakura Finetek, Torrance, CA, U.S.A.), frozen in a plastic mold on dry ice and sectioned in the median plane. The half of each block was immediately frozen in liquid nitrogen for ELISA and Western blot analyses. The other half of the block was cut with a cryomicrotome (Leica, Germany) into 8 μm longitudinal sections containing the epicenter of lesion. These sections were mounted on silane-coated glass slides. The slides were first stained with hematoxylin and eosin (HE) and then with Luxol fast blue and cresyl violet to identify myelin and nerve cells. Sizes of the demyelinated areas in the damaged spinal cords were calculated based on images of the longitudinal sections obtained with image analyzer software (ImageJ version 1.37; National Institutes of Health, Bethesda, MD, U.S.A.).

Sections were incubated in goat serum for 2 hr at room temperature. The sections were then incubated with primary antibodies for 24 hr at 4°C. Primary antibodies against neurofilament (NF160), neuronal nuclei (NeuN) and glial fibrillary acidic protein (GFAP) were used for immunofluorescence staining. Primary antibody binding was detected with anti-mouse Fluor 488 and anti-rabbit Fluor 488 (Invitrogen) antibodies. DAPI (Sigma-Aldrich) was used to stain the nuclei. Tissues were mounted with aqueous mounting medium (Dako Mounting Medium; Dakocytomation, Carpinteria, CA, U.S.A.) and kept in the dark at 4°C until analysis. Fluorescence images were visualized with a confocal microscope (Nikon Corporation, Tokyo, Japan).

Quantitative analysis of inflammatory cytokines and surviving nerves: Segments (1 cm) including the epicenter lesion from the frozen half of the spinal cord were cut and dry-crushed in liquid nitrogen. The tissue powder was used for ELISA and Western blot analysis. The half of powder was suspended in 0.5 m*l* cell extraction buffer (Denaturing Cell Extraction Buffer; Invitrogen) containing a protease inhibitor cocktail (Amresco, Solon, OH, U.S.A.). The clear supernatant was collected after centrifuging twice (10 min, 13,000 *g*, 4°C). IL-6 and COX-2 protein levels in the tissue lysates were also measured using Qunatikine ® canine IL-6 (R&D System, Minneapolis, MN, U.S.A.) and canine COX-2 ELISA (USCN Life Science Inc., Wuhan, China) kits according to the manufacturers' instructions. The plates were measured at a wavelength of 450 nm. Each sample was tested in duplicate.

Half of the powder was used for Western blot analysis. The tissue lysate was suspended in 0.5 m*l* protein extraction buffer (PRO-PREP™ Protein Extraction Solution; iNtRON Biotechnology, Seongnam, South Korea) for 2 hr on ice. Lysates were cleared by twice centrifugation (10 min, 13,000 *g*, 4 °C), and protein concentrations were determined using the Bradford method (Sigma-Aldrich) [5]. Equal amounts of spinal cord protein (30 μg) were separated by 10% sodium dodecyl sulfate polyacrylamide gel electrophoresis and transferred onto polyvinylidene fluoride membranes. The membranes were washed with TBST [10 mM Tris-HCl (pH 7.6), 150 mM NaCl and 0.05% Tween-20], blocked with 5% skim milk for 1 hr and incubated with the appropriate primary antibodies against actin (Sigma-Aldrich), Neuronal Class III β-Tubulin (sc-69966; Tuj1, Santa Cruz Biotechnology), NF-160, NeuN, GalC and GFAP at the recommended dilutions. The membranes were then washed and, primary antibody binding was detected with HRP-conjugated goat anti-rabbit IgG or goat anti-mouse IgG. Bands were visual-

ized with enhanced chemiluminescence (Amersham Pharmacia Biotech, Buckinghamshire, U.K.).

Behavioral assessment: Behavior of the dogs was assessed before SCI and on a weekly basis after the operation to evaluate functional recovery of the hind limbs. Each dog was videotaped from both sides and behind during the neurological examimation. Using Olby scores [51] as well as a revised Tarlov scale and modified Tarlov scale [34], gait was independently scored based on the videotapes by two individuals blinded to the experimental conditions (Table 1). The Basso, Beattie and Bresnahan (B.B.B) scoring system is not appropriate for dogs not capable of plantigrade movement. A mean score was calculated every week following SCI until the 9 weeks study period concluded.

Statistical analysis: Data are presented as the mean ± standard deviation (SD). Statistical analyses were performed using SPSS (version 17.0; SPSS, Chicago, IL, U.S.A.). Differences were analyzed by Kruskal-Wallis and Mann-Whitney U tests. In all statistical analyses, $P<0.05$ was considered to be significant.

RESULTS

Characterization of MSCs derived from fat, BM, WJ, and UCB: Canine MSCs derived from fat, BM, WJ, and UCB showed the same morphology as human MSCs under basal conditions. The canine MSCs formed a monolayer consisting of large and flat cells that developed a spindle-shaped morphology at confluence (Fig. 2). All types of MSCs showed the same phenotype (Fig. 3) with expression of CD44, CD73, CD90 and CD105, and an absence of hematopoietic and endothelial markers including CD14, CD34 and CD45. MSCs derived from fat, BM, WJ and UCB were also able to differentiate into adipocytes and osteoblasts (Fig. 4). The amount of Alizarin red S staining was greater in ADSCs and UCSCs groups than BMSCs and WJSCs groups.

Morphological and phenotypic changes of MSCs after neural induction: After growing in NIM for 72 hr, all MSCs exhibited morphological changes. Most cells retracted their cytoplasm, formed spherical cell bodies and cellular protrusions, and completely stopped proliferating. Finally, MSCs developed a neuronal appearance resulting from neural induction compared to MSCs maintained under normal conditions (Fig. 5). The cells underwent morphological changes as seen by light microscopy (Fig. 5A). We could identify four morphologically distinct subsets of MSCs regardless of their origin (Fig. 5B). About 70–80% of the MSCs appeared as sharp, elongated bi- or tripolar cells with primary, secondary and multi-branched processes (Fig. 5A and 5C). The appearance of the MSCs suggests that they had developed into neurons (black arrowhead), astrocytes (white arrow) or oligodendrocytes (white arrowhead) morphologically. The appearance of percentage of MSCs (15–25%) grown in NIM was similar to that of MSCs grown under basal conditions (Fig. 5A; white arrow) and did not show up-regulation of any neural marker (Fig. 5C; white arrow). There was no significant difference in the development of neural phenotypes among the MSCs groups. Immunofluorescence staining

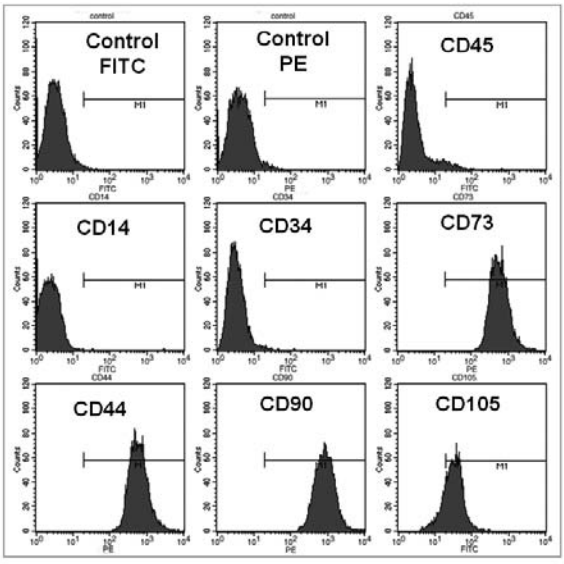

B

	CD14	CD34	CD44	CD45	CD73	CD90	CD105
ADSCs	-	-	+++	-	+++	+++	+++
BMSCs	-	-	+++	-	+++	+++	++
WJSCs	-	-	+++	-	+++	+++	+++
UCSCs	-	-	+++	-	+++	+++	+++

Fig. 3. FACS analysis to assess expressions of CD14, CD34, CD44, CD45, CD73, CD90 and CD105 in MSCs. (A) The expression of cell surface markers in MSCs derived from canine bone marrow. (B) The percentages of the MSCs surface markers are shown as triple-positive, double-positive or negative in the box (+++: more than 95%, ++: more than 80%, −: less than 5%).

showed that the MSCs grown in NIM had high expression of GFAP, GALC, NeuN and NF160 markers (Fig. 5C). The percentage of cells stained with GFAP in UCSCs group was significantly lower than that of WJSCs group. The percentage of cells stained with NeuN in UCSCs group was higher than that of ADSCs group ($P<0.05$).

Histopathological and immunohistochemical analysis: HE and Luxol fast blue staining showed that the demyelinated areas in the MSCs group were significantly smaller than those in the control (Fig. 6A and 6B). The average lesion size of the WJSCs group was larger than other MSC groups, especially the UCSCs group ($P<0.05$). Generalized parenchymal fibrosis and demyelination were more observed at the injured site in the control more frequently (Fig. 6A).

In the longitudinal sections, multifocal funiculi located in the white matter 10 mm apart from the lesion epicenter were found to contain numerous dilated axonal sheaths up to 50 μm in diameter. These frequently contained cellular debris, a few gitter cells (indicating axonal degeneration), and a swollen, round and eosinophilic axon (Fig. 6C and 6D; a_{1-5}). Degeneration and loss of motor neurons were observed

in the spinal cord gray matter 10 mm away caudally from the epicenter. The motor neurons were swollen, chromatolytic and contained karyolytic nuclei (Fig. 6C and 6D; $b_{1–5}$). In the epicenter, scattered groups of reactive astrocytes with a large nucleus and finely stippled chromatin with fibrillar cytoplasm were found (Fig. 6C and 6D; $c_{1–5}$). The lesions contained many plump macrophages with an abundant amount of amphophilic fibrillar cytoplasm that displaced the nucleus to the periphery of the cell. These lesions showed neovascularization at the periphery with macrophage aggregates, and these perivascular infiltrations were composed of a few lymphocytes and many macrophages (Fig. 6C and 6D; $d_{1–5}$). In the MSCs group, residual matrigel was observed with some astrocytosis at the margins (Fig. 6C and 6D; $e_{1–5}$).

The majority of nerve cells at the epicenter of the spinal cord lesion in both the control and MSCs groups died at 8 weeks after transplantation (Fig. 8A). Some surviving nerve cells at the lesion site were positive for NF160, NeuN and GFAP. The morphological features and patterns of the reactive astrocytes observed with immunostaining were similar to those found with light microscopy and HE staining (Fig. 6D; $c_{1–5}$).

Transplanted MSCs in the injured spinal cord were identified by the presence of fluorescent nanoparticles in the cytoplasm, but these cells were not found at cranial or caudal injection sites of the spinal cords. Some MSCs (Fig. 8) expressed markers for neurons (NF160), neuronal nuclei (NeuN) and astrocytes (GFAP). Interestingly, NF160- and NeuN-positive neurons were found more in the MSCs groups than the control animals, but GFAP-positive reactive astrocytes were observed more often in the control group than in MSCs groups (Fig. 8). The number of surviving MSCs in BMSCs group was less than that in other MSCs groups, although the same number of MSCs was transplanted into each group.

Surviving nerve cells and axons were found within residual matrigel (Fig. 8; d), and numerous UCSCs migrated to the margin of the matrigel (Fig. 8; o). Active astrocytes of MSCs groups were more focalized than those of the control except for ones from the BMSCs group, while endogenous progenitor cells of the control group diffusely differentiated into active astrocytes (Fig. 8; k–o). In high magnification images, the axons of the control animals were found to be shorter and more disconnected than those of the MSCs groups at 8 weeks after transplantation (Fig. 8; a–e). Some MSCs surrounded the surviving axon and differentiated neuronal cells having long and synaptic nerve chain (Fig. 8; b', e'). But, very few MSCs expressed neurofilament marker (Fig. 8; b–e). A few MSCs contained neural nuclei (Fig. 8; g–j).

Anti-inflammatory effects and neuronal regeneration: To quantitatively evaluate the anti-inflammation effects and neuronal regeneration in spinal cord injured site, ELISA was performed. The protein levels of COX-2 and IL-6 (two inflammatory cytokines) were significantly decreased in the MSCs groups compared to the control group ($P<0.05$, Fig. 7). There was no difference in IL-6 protein levels among the MSCs groups, but the COX-2 protein level in UCSCs group was significantly lower than the other MSCs groups ($P<0.05$).

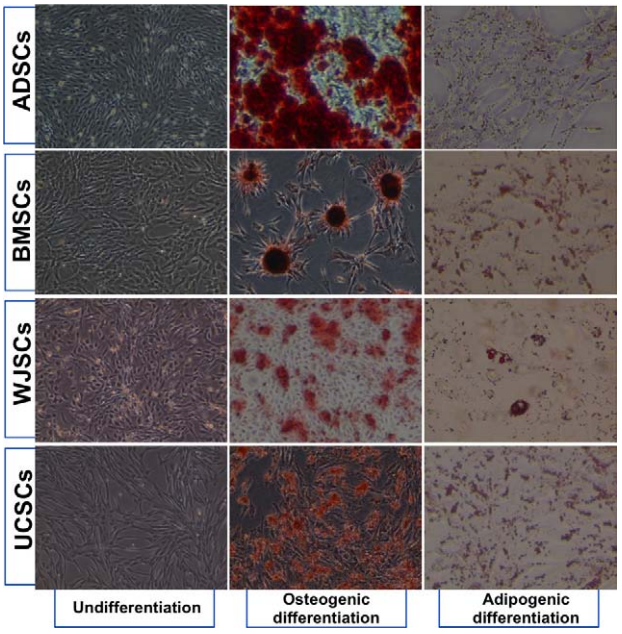

Fig. 4. Osteogenic and adipogenic differentiations of MSCs. Canine MSCs derived from fat (ADSCs), bone marrow (BMSCs), Wharton's jelly (WJSCs), and umbilical cord blood (UCSCs) grown in basal conditions had morphologies similar to human MSCs. The presence of mineralized bone matrix deposits was confirmed by Alizarin red staining, and lipid-containing vacuoles were identified by Oil red O staining at passage three.

Western blot analysis revealed that the levels of Tuj1, NF160, NeuN, GALC and GFAP proteins were altered in a manner similar to what was found by histological and confocal microscopic analysis (Fig. 9). The expressions of Tuj1, NF160, NeuN and GALC were reduced in the control injured cords compared to spinal cords containing MSCs. However, the levels of GFAP protein in the injured cords of MSCs groups were significantly lower than those of the control group ($P<0.05$, Fig. 9). In UCSCs group, the expressions of Tuj1, NF160 and NeuN were significantly increased, and the level of GFAP was significantly decreased compared to other MSCs groups ($P<0.05$).

Behavioral outcomes: Prior to spinal cord occlusion, all experimental dogs had a score of 14 on the Olby score and 9 on the revised modified Tarlov scale. All injured dogs showed complete pelvic limb paralysis after SCI (Fig. 10). The Olby test scores of control group gradually increased during the study period. However, their scores were maintained around 3 points which represented possible minimal nonweight-bearing protraction of the pelvic limb in only one joint throughout the 8 weeks of the study period (Fig. 10A). In the MSCs groups, Olby scores increased to 5–6 points which indicated possible weight-bearing protraction of pelvic limb less than 10% at 8 weeks after transplantation. The mobility of the MSCs groups was significantly greater than that of the control group after 2 weeks *(P*<0.05).

Functional motor outcomes were also assessed based on

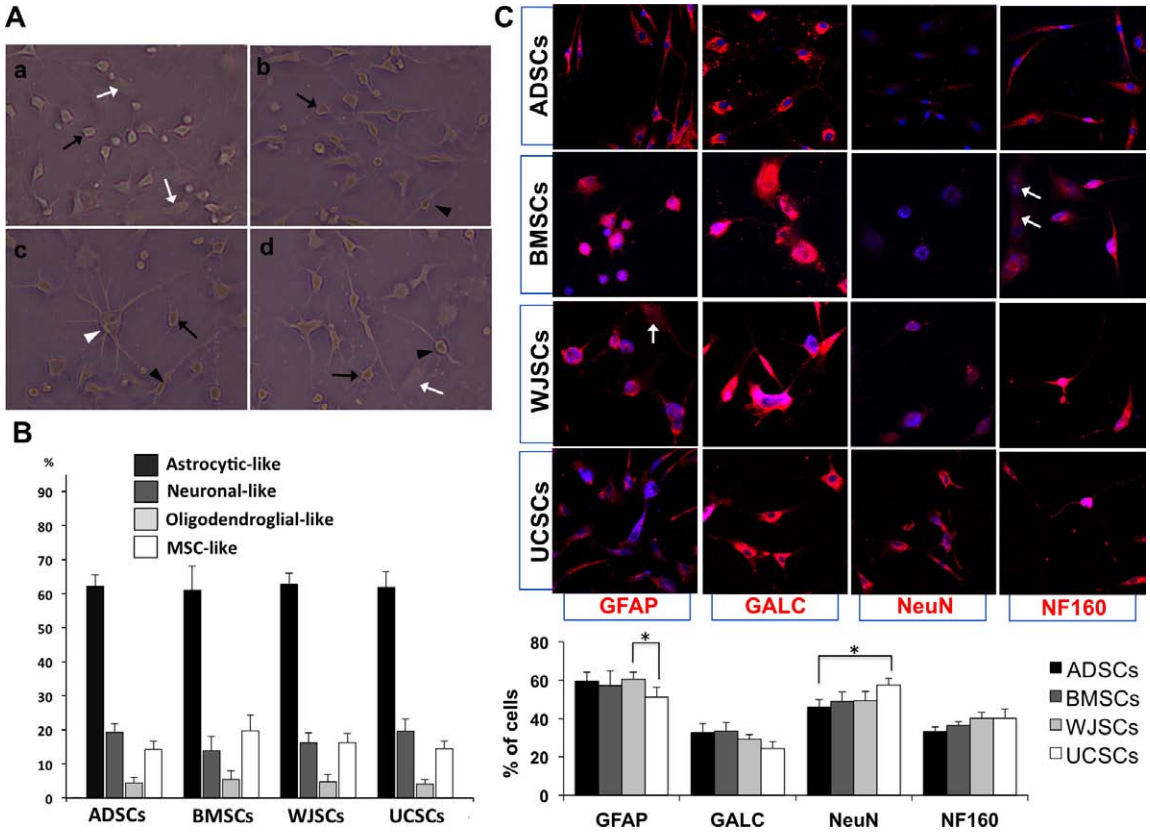

Fig. 5. Morphologic changes following neuronal induction of MSCs. After growing in neural induction medium for 72 hr, all MSCs exhibited morphological changes. Most cells retracted their cytoplasm, forming spherical cell bodies and emitted cellular protrusions. (A) Neural morphology of MSCs was observed by light microscopy; (a) ADSCs, (b) BMSCs, (c) WJSCs, (d) UCSCs. Neurons (black arrowhead) appeared as sharp, elongated and bipolar cells. Astrocytes (white arrow) appeared as tripolar or multipolar cells with primary processes. Oligodendrocytes (white arrowhead) appeared as multipolar cells with secondary and multi-branched processes. Undifferentiated MSCs (white arrow) appeared as spindle cells with abundant cytoplasm. (B) We identified four morphologically distinct subsets of neuronal MSCs regardless of their origin. About 70–80% of the MSCs appeared as neurons, astrocytes or oligodendrocytes. There were no differences in the number of different neural cells types observed among the groups of MSCs. (C) Although, some of MSCs (white arrow) remained undifferentiated and did not up-regulate the expression of any neural markers, MSCs showed intense staining for GFAP, GALC, NeuN and NF160. *P<0.05 comparison between two groups.

the revised modified Tarlov scale (Fig. 10B). Scores for the MSCs groups increased to 3–4 points at 8 weeks after transplantation. Neurologic recovery in MSCs groups differed significantly from that in control group at 2 weeks following MSC transplantation (P<0.05). All dogs in the MSCs groups had purposeful hind limb motion, and 62.5% of them (10/16) were able to stand with some assistance at 8 weeks after transplantation. No significant differences were observed among the MSCs groups.

DISCUSSION

All MSCs derived from the four different sources exhibited typical MSC characteristics: a fibroblastoid morphology, multipotential differentiation capability and expression of a characteristic set of surface proteins. MSCs derived from the four sources expressed classic MSC markers including CD44, CD73, CD90 and CD105 as other studies described [10, 16, 35, 48]. Our study found that ADSCs, BMSCs, WJSCs and UCSCs all possessed a multilineage differentiation capacity. All MSCs differentiated into both osteogenic and adipogenic lineages. However, MSCs could not produce an intense lipid droplet, which was related to the short 2 weeks differentiation period. During neural differentiation, MSCs not only underwent nerve cell-like morphological changes *in vitro*, but also expressed neural cell markers. MSCs developed rounded cell bodies with bipolar or multipolar neurite-like extensions similar to neural stem cells. The neuron-like MSCs also stained positive for several neural proteins including GFAP, GALC, NeuN and NF160, which indicated that these populations consisted of progenitor astrocytes, oligodendrocytes and neurons. However, morphological changes and increases in immunofluoresence stain for neuronal markers upon chemical induction of MSCs *in vitro* were likely the result of cellular toxicity and cell shrinkage [23]. So, the fate of transplanted MSCs

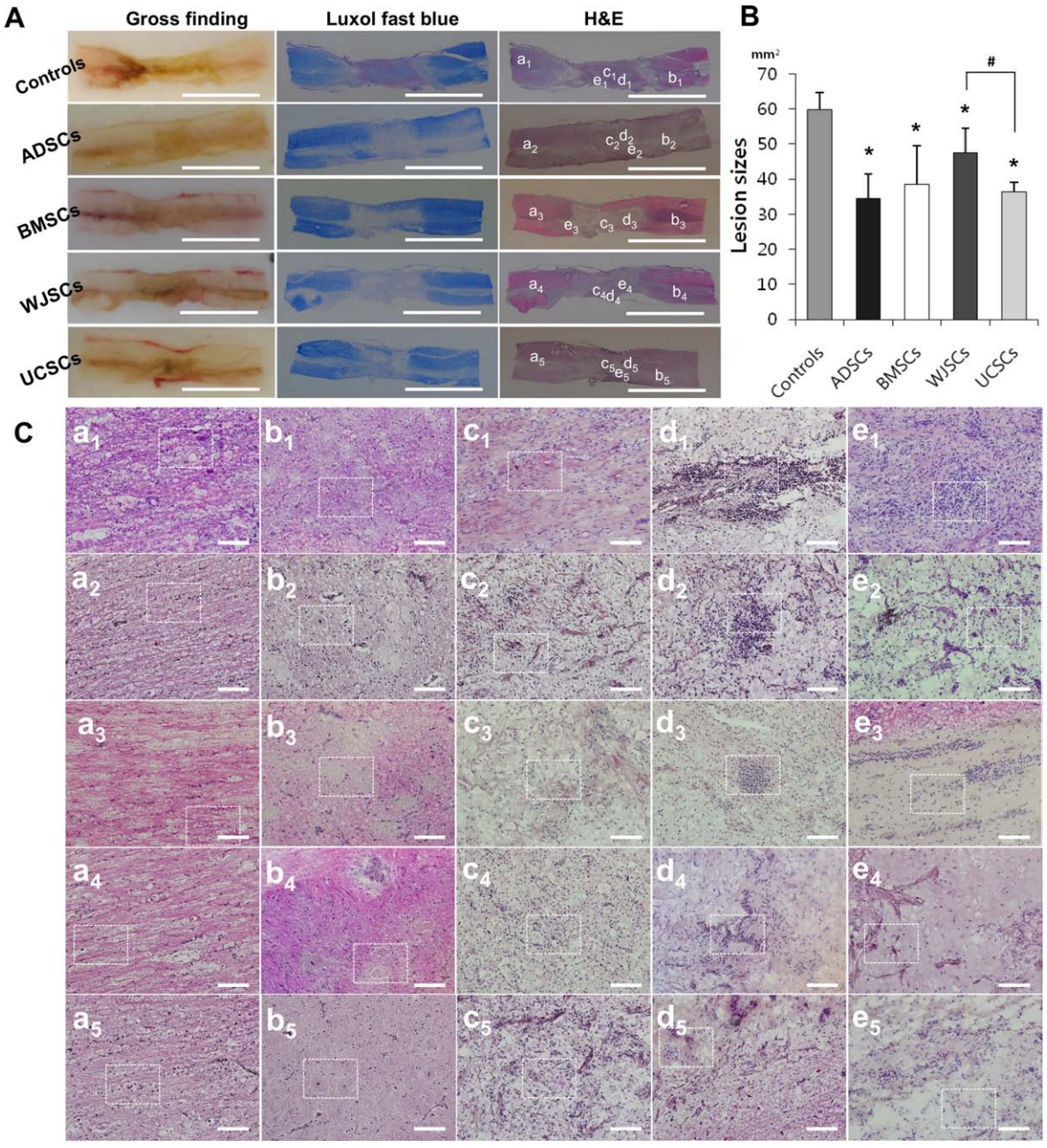

in injured spinal cord is most important criteria to evaluate their potentials of neuronal differentiation.

The fate of transplanted cells is determined by the environment into which the cells are transplanted rather than intrinsic properties of the cells [13, 18]. The ideal environment for transplanted MSCs depends on the type of SCI along with the time and method of transplantation. We used a clinically-relevant experimental model of balloon compression SCI. In animal models, contusion and transection injuries are induced by spinal cord exposure during laminectomy, while balloon compression injuries occur in an enclosed environment [39]. Compression injury results in neuronal apoptosis at the lesion site beginning at 6 hr and persisting for at least 3 weeks post-injury [7, 42]. Compression injury is also accompanied by a prolonged secondary inflammatory response [4] that activates resident microglia and macrophages which may lead to phagocytosis of myelin debris [33, 43]. In contrast, transection of the spinal cord results in a narrow zone of primary tissue damage that is followed by a focal secondary pathological and inflammatory responses [43].

In the present study, MSCs with matrigel were transplanted into the parenchyma of the spinal cord near the lesion site (cranial and caudal) and directly into the injury epicenter at 7 days post injury (dpi). This method has three main benefits.

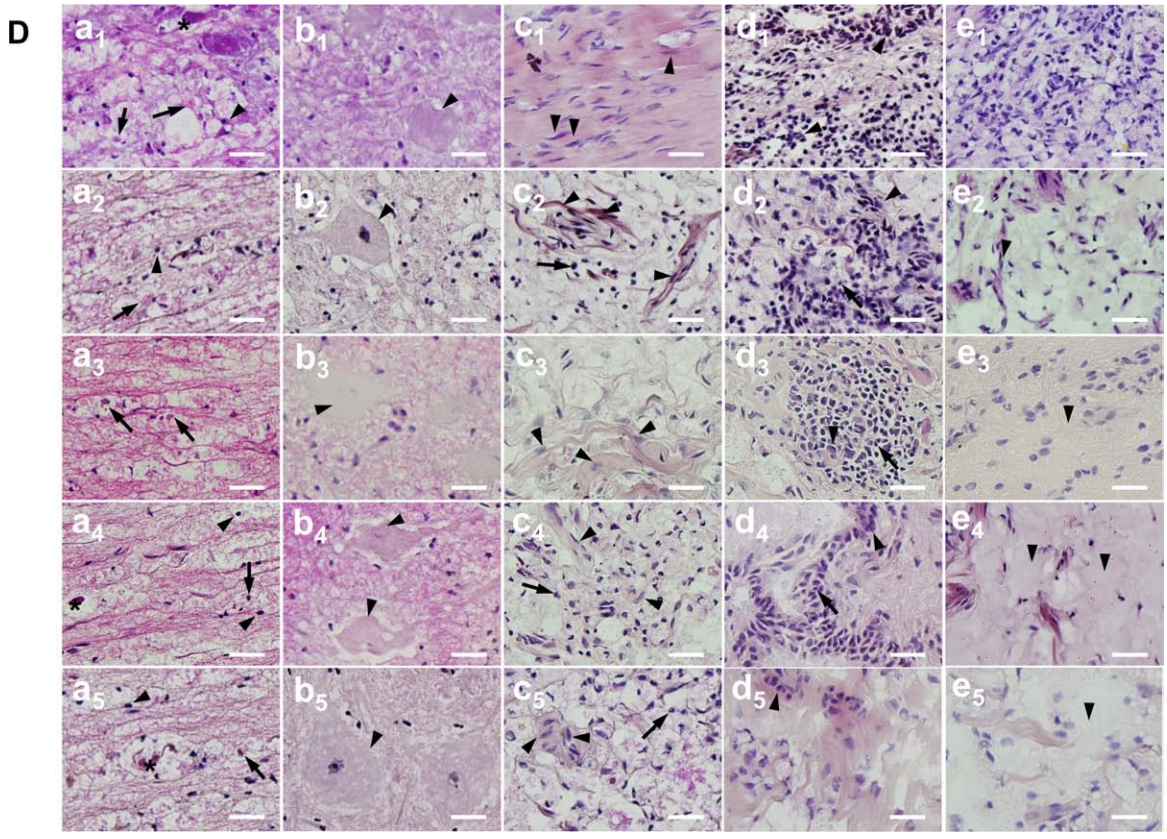

Fig. 6. [Left page] (A) Representative longitudinal sections of injured spinal cord from each MSCs group. Longitudinal sections showed fibrosis, hemorrhage and demyelinated lesions in HE and Luxol fast blue stain (the left side is rostral). Hemorrhage and fibrosis were identified by reddish and brownish lesions. a_{1-5}: in the white matter, b_{1-5}: in the gray matter, c_{1-5}: fibrosis in the epicenter, d_{1-5}: inflammatory cell infiltration into epicenter, e_{1-5}: residual scaffolds in the epicenter. (B) MSCs transplants reduced the spinal cord lesion size. *P<0.05 compared to the control. #P<0.05 comparison between two groups. (C) Images of the marked lesions in panel (A). [This page] (D) High magnification images are shown in the white box in (C); a_{1-5}: white matter; Most of the cells in the image are oligodendrocytes with dark round nuclei; some of the cells are astrocytes. White matter funiculi were composed of numerous dilated axonal sheaths which frequently contain cellular debris and gitter cells. Astrogliosis (arrowhead), gitter cells (arrow), and spheroids (asterisk). b_{1-5}: Degenerative neurons (arrowhead) were shown in gray matter. c_{1-5}: Fibrosis in the epicenter; astrogliosis (arrow) and reactive astrocytes (arrowhead). d_{1-5}: Inflammatory infiltration in the epicenter; macrophages (arrowhead) and lymphocytes (arrow). e_{1-5}: Residual scaffolds (matrigel); some astrocytosis was found at the margins of the matrigel (arrowhead). The scale bar in (A) is equal to 10 mm, the scale bar in (C) is equal to 100 μm, and scale bar in (D) is equal to 25 μm, respectively.

The first involves cavity formation at the lesion epicenter after SCI [24]. Matrigel maintains the microenvironment as a cellular bridge at the site where cavity formation is predicted to occur. This material also exerts effects that promote transplantation including rescuing dying cells, increasing cell proliferation, blocking inflammatory and cytotoxic cytokines, and promoting neuronal differentiation [25, 49]. The second benefit is that transplantation at 7 dpi may increase survival rate of transplanted MSCs and dramatically modulate inflammation in the spinal cord. The success of cell transplantation is critically dependent on the time of cell injection [28, 31] relative to the development of neurotoxicity caused by inflammatory cytokines during the acute phase and a cystic cavity which prevents axonal regeneration during the chronic phase [27]. Cell survival is increased when the cells are transplanted during the subacute phase of SCI rather than the acute phase [29]. Furthermore, the lesion is not fully developed at 7 dpi, so transplanted MSCs may act as a neuroprotective agent. The third benefit, the presence of phagocytic cell populations at the injury site suggests that the epicenter may not be a favorable environment for cell survival [4]. Therefore, we transplanted MSCs into relatively normal parenchyma (cranial and caudal) adjacent to the lesion site and epicenter to increase MSC survival.

This study focused on the survival and integration of allogenic MSCs in the injured spinal cord, and identified which MSCs contribute to functional recovery. Our results demonstrated that allogenic MSCs can be successfully survived in injured spinal cords where they integrated into host tissue without immunosuppressive agents [28, 36] and MSCs also improved hind-limb function following SCI. Many reports have also described MSCs as having immunosuppres-

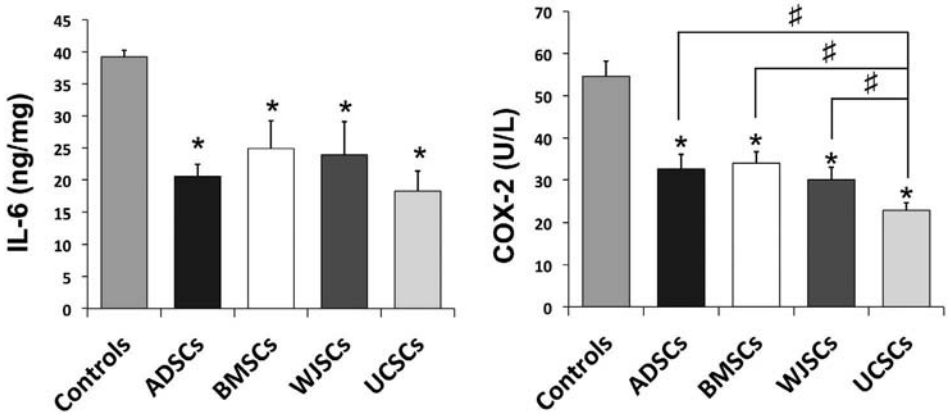

Fig. 7. The expression of COX-2 and IL-6 at 8 weeks after transplantation of MSCs. COX-2 and IL-6 protein levels in MSCs groups were lower than those in the control group. Especially, COX-2 protein level in UCSCs group was the lowest than that in other groups. **P*<0.05 compared with control. #*P*<0.05 compared between two groups.

sive properties, and that MSCs can modulate many T-cell functions [3, 9]. However, others have used the high dose of cyclosporine as an immunosuppressive drug, and some studies have found cyclosporine to be effective in improving survival of stem cell after transplantation into injured spinal cord [30, 45]. Therefore, MSCs transplantation with immnunosuppressive drugs should be considered in further study and clinical treatment.

We observed reduced levels of reactive astrogliosis and macrophage infiltration into the lesion epicenter in the MSCs groups. Especially, COX-2 protein expression in the UCSCs group was significantly decreased compared to the other MSCs groups. MSC transplantation modulates neuroinflammation by reducing the expression of proinflammatory cytokine such as COX-2 and IL-6 and subsequently prevents astrocytosis [6, 26]. Astrocytes are both the target and the source of neuroinflammation. These cells are stimulated by mediators released from microglia, down-regulate the expression of neurotrophic factors and release additional inflammatory mediators which in turn further activate microglia [4]. The reduced number of GFAP-positive astrocytes indicated a possible deleterious effect of astrocytes, perhaps because these cells contributed to glial scarring. Although a low number of MSCs differentiated into astrocytes in the lesion core, these astrocytes did not appear to participate in a typical glial scarring reaction as indicated both by their morphology and reduced GFAP expression.

MSCs were transplanted into injured spinal cords to evaluate their potential neuroprotection and neuronal regeneration effects associated with SCI repair. Many MSCs can survive following transplantation, but very few MSCs can transform into neural-like cells *in vivo*. Most of NF160- and NeuN-positive neurons at injured spinal cord were derived from endogenous spinal cord-derived neural progenitor cells or preserved neurons due to neuroprotection and anti-inflammatory effects of transplanted MSCs. Based on the rapid recovery after MSC transplantation observed in this study, cell replacement unlikely explains this improvement in functional outcome following SCI [54]. Many of the studies that have reported functional improvement with MSC transplantation do so soon after the first 2 or 3 weeks after injury [17, 46], suggesting that the MSCs have neuroprotective rather than a regenerative effects. Western blot analysis revealed that the amount of protein positive for Tuj1, NF160, NeuN and GALC was higher in the MSCs groups. In UCSCs group, the expressions of Tuj1, NF160 and NeuN were significantly increased, and the level of GFAP was significantly decreased compared to other MSCs groups. Although the mechanism of more neuroprotection effect in UCSCs group is still unclear but may related with anti-inflammation factor involved in down regulation of COX-2 in injured spinal cord. Anti-inflammatory factors of engrafted UCSCs play important roles in proliferation, migration and differentiation of endogenous spinal cord-derived neural progenitor cells in an injured region.

Some of the MSCs were found close to neurons and axon, where MSCs can deliver trophic and immunomodulatory factors to neural progenitor cells and surviving neural cells. The ability of neural progenitor cells to secrete a variety of neurotrophic factors indicates that they could promote the growth of damaged axons [22]. The level of neurotrophic factors decreases after neuronal differentiation [21]. In our study, the majority of transplanted MSCs remained undifferentiated. Before and during neural differentiation, MSCs can produce vascular endothelial growth factor and brain-derived neurotrophic factor, which are known to have neuroprotective effects in SCI lesions [15, 21].

Although UCSCs provided greater levels of neuroprotection to the surviving neural cells in the SCI lesions, functional recovery was not significantly different among the MSCs groups. Functional recovery up to the next stage with our scoring system, which is possible that dogs can stand without assistance, is quite different from the scored in this study which are able to stand with assistance. We believe the reason for the poor correlation between neuroprotection and functional recovery is that increased axons and nerve cells

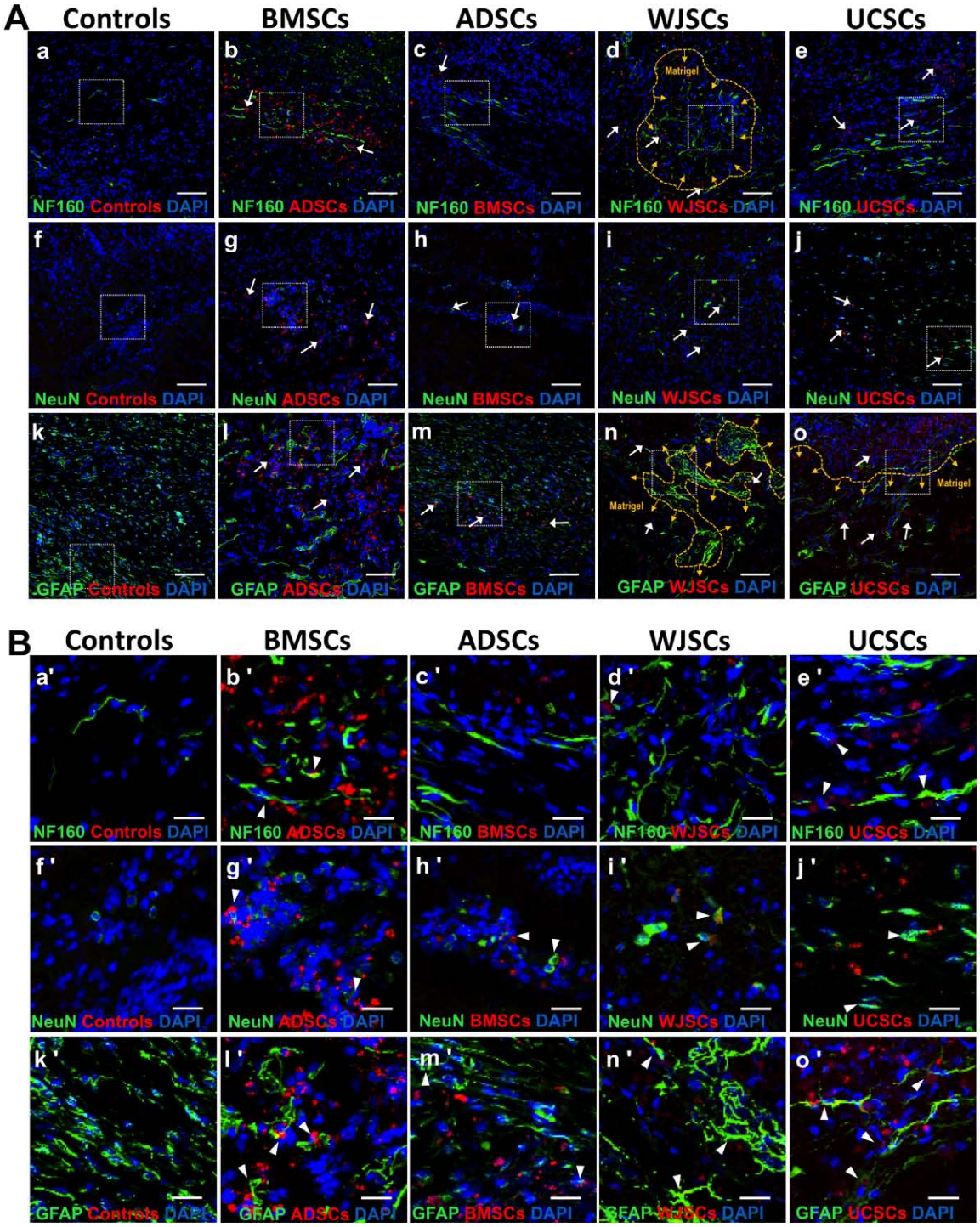

Fig. 8. (A) Surviving MSCs in the epicenter stained for neural markers. MSCs in the injured spinal cord at 8 weeks following transplantation could be identified by the appearance of fluorescent nanoparticles (red) in the cytoplasm viewed by confocal microscopy. Some (arrowheads) MSCs expressed markers for neurons (NF160), neuronal nuclei (NeuN) and astrocytes (GFAP). (a–e) More shortened and disconnected axons were observed in control group than in the MSCs groups at 8 weeks. (d) and (d') Surviving nerve cells and axonal growth were observed within the residual matrigel. (k–o) and (k'–o') Morphological features and patterns of reactive astrocyte were similar to those observed with HE staining under light microscopy (Fig. 6D; c_{1-5}). (o) and (o') Migration of numerous UCSCs was observed at the margin of matrigel. (b'–e') Some MSCs surrounded surviving axons but very few MSCs expressed neurofilament marker. (g'–j') Some MSCs contained neural nuclei. The scale bars in (a–o) and (a'–o') are equal to 100 and 25 μm, respectively.

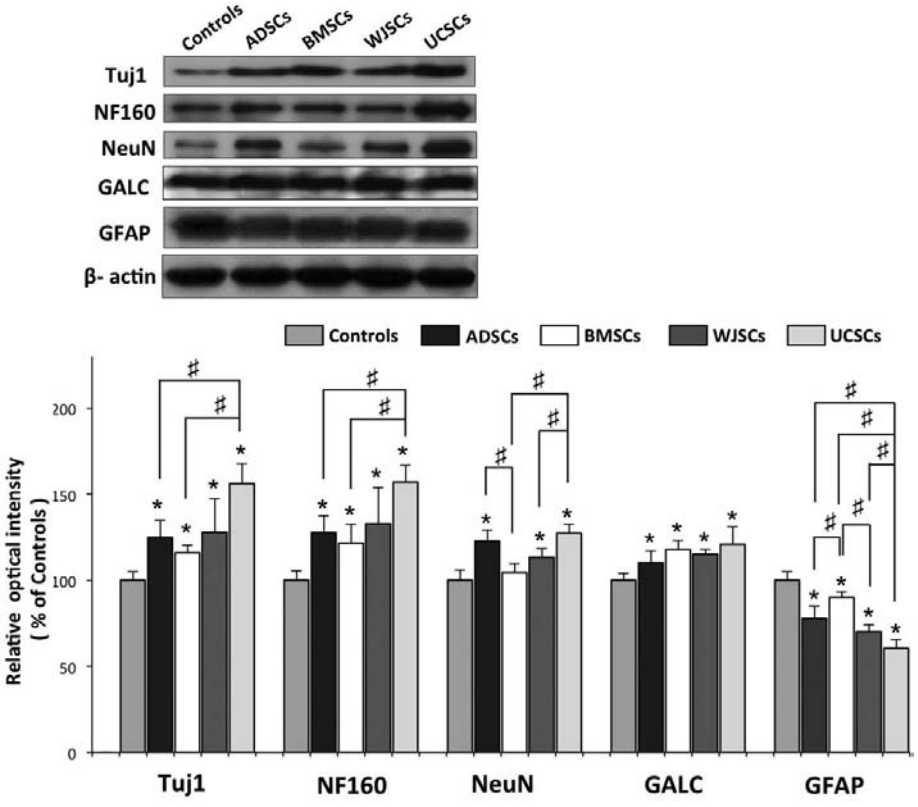

Fig. 9. Western blot analysis of Tuj1, NF160, NeuN, GALC and GFAP expression in injured spinal cords. The levels of Tuj1, NF160, Neu, and GALC were increased in the injured cords compared to control group. The levels of GFAP protein in the MSCs groups were significantly lower than those of the control group (P<0.05). *P<0.05 compared with control. #P<0.05 compared between two groups.

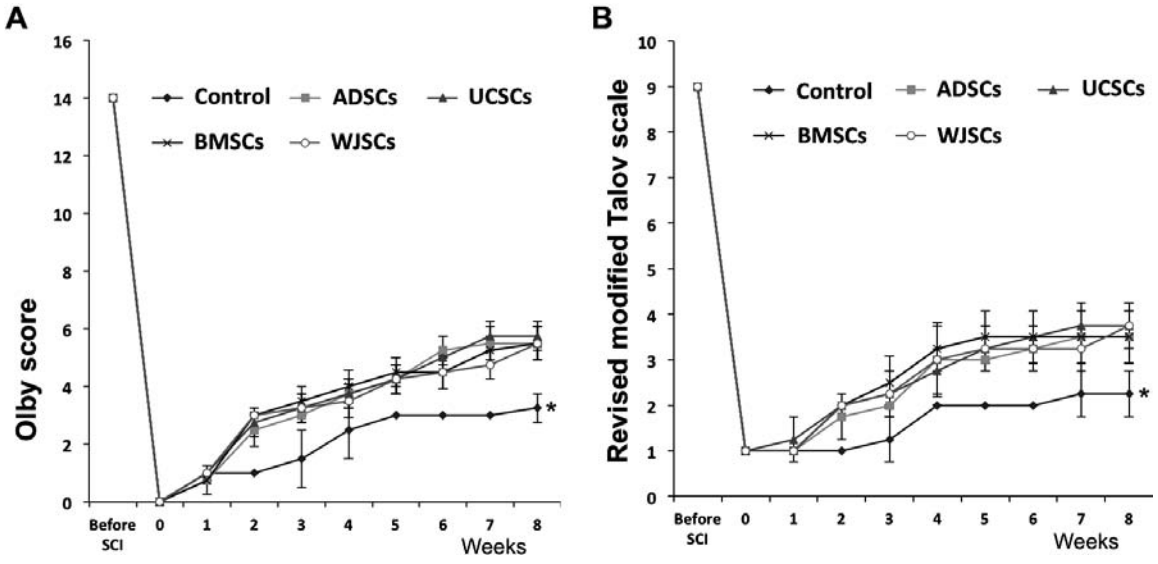

Fig. 10. Behavioral analysis following transplantation. All injured dogs showed complete pelvic limb paralysis after SCI. Neurologic recovery differed significantly among groups from 2 weeks following transplantation (P<0.05). (A) Olby scores (B) Revised modified Tarlov scale. There were no significant differences in functional recovery among the MSCs groups. *P<0.05 compared with MSCs group.

were not properly rearranged for normal nerve conduction. More normal neural cells in the lesion site may have been needed to obtain higher functional recovery rates.

In conclusion, MSCs derived from fat, BM, WJ and UCB promote functional recovery after SCI. UCSCs were associated with more nerve regeneration, neuroprotection and less inflammation than other MSCs. Additionally, matrigel with MSCs could act as a cellular bridge and assist axon growth at the injury site. Our results demonstrated that implanted MSCs survive and migrate toward neural cells at injured site and help preserve axon and neural cells, thus resulting in improved hind-limb function following SCI.

ACKNOWLEDGMENTS. This work was supported by the National Research Foundation of Korea (NRF) grant funded by the Korea government (MEST) (No. 20090077045), the Research Institute for Veterinary Science of Seoul National University and by a grant from the Next-Generation BioGreen 21 program (No.P J008030, J008032), Rural Development Administration, Republic of Korea.

REFERENCES

1. Akiyama, Y., Honmou, O., Kato, T., Uede, T., Hashi, K. and Kocsis, J. D. 2001. Transplantation of clonal neural precursor cells derived from adult human brain establishes functional peripheral myelin in the rat spinal cord. *Exp. Neurol.* **167**: 27–39. [Medline] [CrossRef]
2. Barnett, S. C. and Riddell, J. S. 2007. Olfactory ensheathing cell transplantation as a strategy for spinal cord repair-what can it achieve? *Nat. Clin. Pract. Neurol.* **3**: 152–161. [Medline] [CrossRef]
3. Bartholomew, A., Sturgeon, C., Siatskas, M., Ferrer, K., McIntosh, K., Patil, S., Hardy, W., Devine, S., Ucker, D., Deans, R., Moseley, A. and Hoffman, R. 2002. Mesenchymal stem cells suppress lymphocyte proliferation *in vitro* and prolong skin graft survival *in vivo*. *Exp. Hematol.* **30**: 42–48. [Medline] [CrossRef]
4. Beck, K. D., Nguyen, H. X., Galvan, M. D., Salazar, D. L., Woodruff, T. M. and Anderson, A. J. 2010. Quantitative analysis of cellular inflammation after traumatic spinal cord injury: evidence for a multiphasic inflammatory response in the acute to chronic environment. *Brain* **133**: 433–447. [Medline] [CrossRef]
5. Bradford, M. M. 1976. A rapid and sensitive method for the quantitation of microgram quantities of protein utilizing the principle of protein-dye binding. *Anal. Biochem.* **72**: 248–254. [Medline] [CrossRef]
6. Carlson, N. G., Rojas, M. A., Redd, J. W., Tang, P., Wood, B., Hill, K. E. and Rose, J. W. 2010. Cyclooxygenase-2 expression in oligodendrocytes increases sensitivity to excitotoxic death. *J. Neuroinflammation* **7**: 25. [Medline] [CrossRef]
7. Crowe, M. J., Bresnahan, J. C., Shuman, S. L., Masters, J. N. and Beattie, M. S. 1997. Apoptosis and delayed degeneration after spinal cord injury in rats and monkeys. *Nat. Med.* **3**: 73–76. [Medline] [CrossRef]
8. Dasari, V. R., Spomar, D. G., Gondi, C. S., Sloffer, C. A., Saving, K. L., Gujrati, M., Rao, J. S. and Dinh, D. H. 2007. Axonal remyelination by cord blood stem cells after spinal cord injury. *J. Neurotrauma* **24**: 391–410. [Medline] [CrossRef]
9. Di Nicola, M., Carlo-Stella, C., Magni, M., Milanesi, M., Longoni, P. D., Matteucci, P., Grisanti, S. and Gianni, A. M. 2002. Human bone marrow stromal cells suppress T-lymphocyte proliferation induced by cellular or nonspecific mitogenic stimuli. *Blood* **99**: 3838–3843. [Medline] [CrossRef]
10. Erices, A., Conget, P. and Minguell, J. J. 2000. Mesenchymal progenitor cells in human umbilical cord blood. *Br. J. Haematol.* **109**: 235–242. [Medline] [CrossRef]
11. Fawcett, J. W. and Asher, R. A. 1999. The glial scar and central nervous system repair. *Brain Res. Bull.* **49**: 377–391. [Medline] [CrossRef]
12. Frisen, J., Johansson, C. B., Torok, C., Risling, M. and Lendahl, U. 1995. Rapid, widespread, and longlasting induction of nestin contributes to the generation of glial scar tissue after CNS injury. *J. Cell Biol.* **131**: 453–464. [Medline] [CrossRef]
13. Gorio, A., Torrente, Y., Madaschi, L., Di Stefano, A. B., Pisati, F., Marchesi, C., Belicchi, M., Di Giulio, A. M. and Bresolin, N. 2004. Fate of autologous dermal stem cells transplanted into the spinal cord after traumatic injury (TSCI). *Neuroscience* **125**: 179–189. [Medline] [CrossRef]
14. Han, H. J., Sigurdson, W. J., Nickerson, P. A. and Taub, M. 2004. Both mitogen activated protein kinase and the mammalian target of rapamycin modulate the development of functional renal proximal tubules in matrigel. *J. Cell Sci.* **117**: 1821–1833. [Medline] [CrossRef]
15. Hardy, S. A., Maltman, D. J. and Przyborski, S. A. 2008. Mesenchymal stem cells as mediators of neural differentiation. *Curr. Stem Cell Res. Ther.* **3**: 43–52. [Medline] [CrossRef]
16. Hauner, H., Entenmann, G., Wabitsch, M., Gaillard, D., Ailhaud, G., Negrel, R. and Pfeiffer, E. F. 1989. Promoting effect of glucocorticoids on the differentiation of human adipocyte precursor cells cultured in a chemically defined medium. *J. Clin. Invest.* **84**: 1663–1670. [Medline] [CrossRef]
17. Hofstetter, C. P., Schwarz, E. J., Hess, D., Widenfalk, J., El Manira, A., Prockop, D. J. and Olson, L. 2002. Marrow stromal cells form guiding strands in the injured spinal cord and promote recovery. *Proc. Natl. Acad. Sci. U.S.A.* **99**: 2199–2204. [Medline] [CrossRef]
18. Johansson, C. B., Momma, S., Clarke, D. L., Risling, M., Lendahl, U. and Frisen, J. 1999. Identification of a neural stem cell in the adult mammalian central nervous system. *Cell* **96**: 25–34. [Medline] [CrossRef]
19. Kang, S. K., Shin, M. J., Jung, J. S., Kim, Y. G. and Kim, C. H. 2006. Autologous adipose tissue-derived stromal cells for treatment of spinal cord injury. *Stem Cells Dev.* **15**: 583–594. [Medline] [CrossRef]
20. Kleinman, H. K., McGarvey, M. L., Hassell, J. R., Star, V. L., Cannon, F. B., Laurie, G. W. and Martin, G. R. 1986. Basement membrane complexes with biological activity. *Biochemistry* **25**: 312–318. [Medline] [CrossRef]
21. Koh, S. H., Kim, K. S., Choi, M. R., Jung, K. H., Park, K. S., Chai, Y. G., Roh, W., Hwang, S. J., Ko, H. J., Huh, Y. M., Kim, H. T. and Kim, S. H. 2008. Implantation of human umbilical cord-derived mesenchymal stem cells as a neuroprotective therapy for ischemic stroke in rats. *Brain Res.* **1229**: 233–248. [Medline] [CrossRef]
22. Llado, J., Haenggeli, C., Maragakis, N. J., Snyder, E. Y. and Rothstein, J. D. 2004. Neural stem cells protect against glutamate-induced excitotoxicity and promote survival of injured motor neurons through the secretion of neurotrophic factors. *Mol. Cell. Neurosci.* **27**: 322–331. [Medline] [CrossRef]
23. Lu, P., Blesch, A. and Tuszynski, M. H. 2004. Induction of bone marrow stromal cells to neurons: differentiation, transdifferentiation, or artifact? *J. Neurosci. Res.* **77**: 174–191. [Medline] [CrossRef]
24. McTigue, D. M., Tani, M., Krivacic, K., Chernosky, A., Kelner, G. S., Maciejewski, D., Maki, R., Ransohoff, R. M. and Stokes, B. T. 1998. Selective chemokine mRNA accumulation in the rat

spinal cord after contusion injury. *J. Neurosci. Res.* **53**: 368–376. [Medline]
25. Mirza, B., Krook, H., Andersson, P., Larsson, L. C., Korsgren, O. and Widner, H. 2004. Intracerebral cytokine profiles in adult rats grafted with neural tissue of different immunological disparity. *Brain Res. Bull.* **63**: 105–118. [Medline] [CrossRef]
26. Okada, S., Nakamura, M., Mikami, Y., Shimazaki, T., Mihara, M., Ohsugi, Y., Iwamoto, Y., Yoshizaki, K., Kishimoto, T., Toyama, Y. and Okano, H. 2004. Blockade of interleukin-6 receptor suppresses reactive astrogliosis and ameliorates functional recovery in experimental spinal cord injury. *J. Neurosci. Res.* **76**: 265–276. [Medline] [CrossRef]
27. Okano, H. 2002. Stem cell biology of the central nervous system. *J. Neurosci. Res.* **69**: 698–707. [Medline] [CrossRef]
28. Park, S. S., Byeon, Y. E., Ryu, H. H., Kang, B. J., Kim, Y., Kim, W. H., Kang, K. S., Han, H. J. and Kweon, O. K. 2011. Comparison of canine umbilical cord blood-derived mesenchymal stem cell transplantation times: involvement of astrogliosis, inflammation, intracellular actin cytoskeleton pathways, and neurotrophin. *Cell Transplant.* **20**: 1867–1880. [Medline]
29. Parr, A. M., Kulbatski, I. and Tator, C. H. 2007. Transplantation of adult rat spinal cord stem/progenitor cells for spinal cord injury. *J. Neurotrauma* **24**: 835–845. [Medline] [CrossRef]
30. Parr, A. M., Kulbatski, I., Wang, X. H., Keating, A. and Tator, C. H. 2008. Fate of transplanted adult neural stem/progenitor cells and bone marrow-derived mesenchymal stromal cells in the injured adult rat spinal cord and impact on functional recovery. *Surg. Neurol.* **70**: 600–607. [Medline] [CrossRef]
31. Pearse, D. D. and Bunge, M. B. 2006. Designing cell- and gene-based regeneration strategies to repair the injured spinal cord. *J. Neurotrauma* **23**: 438–452. [Medline] [CrossRef]
32. Pittenger, M. F., Mackay, A. M., Beck, S. C., Jaiswal, R. K., Douglas, R., Mosca, J. D., Moorman, M. A., Simonetti, D. W., Craig, S. and Marshak, D. R. 1999. Multilineage potential of adult human mesenchymal stem cells. *Science* **284**: 143–147. [Medline] [CrossRef]
33. Popovich, P. G., Wei, P. and Stokes, B. T. 1997. Cellular inflammatory response after spinal cord injury in Sprague-Dawley and Lewis rats. *J. Comp. Neurol.* **377**: 443–464. [Medline] [CrossRef]
34. Rabinowitz, R. S., Eck, J. C., Harper, C. M. Jr., Larson, D. R., Jimenez, M. A., Parisi, J. E., Friedman, J. A., Yaszemski, M. J. and Currier, B. L. 2008. Urgent surgical decompression compared to methylprednisolone for the treatment of acute spinal cord injury: a randomized prospective study in beagle dogs. *Spine (Phila Pa 1976)* **33**: 2260–2268. [Medline] [CrossRef]
35. Reyes, M., Lund, T., Lenvik, T., Aguiar, D., Koodie, L. and Verfaillie, C. M. 2001. Purification and *ex vivo* expansion of postnatal human marrow mesodermal progenitor cells. *Blood* **98**: 2615–2625. [Medline] [CrossRef]
36. Ryu, H. H., Lim, J. H., Byeon, Y. E., Park, J. R., Seo, M. S., Lee, Y. W., Kim, W. H., Kang, K. S. and Kweon, O. K. 2009. Functional recovery and neural differentiation after transplantation of allogenic adipose-derived stem cells in a canine model of acute spinal cord injury. *J. Vet. Sci.* **10**: 273–284. [Medline] [CrossRef]
37. Safford, K. M., Hicok, K. C., Safford, S. D., Halvorsen, Y. D., Wilkison, W. O., Gimble, J. M. and Rice, H. E. 2002. Neurogenic differentiation of murine and human adipose-derived stromal cells. *Biochem. Biophys. Res. Commun.* **294**: 371–379. [Medline] [CrossRef]
38. Sasaki, M., Radtke, C., Tan, A. M., Zhao, P., Hamada, H., Houkin, K., Honmou, O. and Kocsis, J. D. 2009. BDNF-hypersecreting human mesenchymal stem cells promote functional recovery, axonal sprouting, and protection of corticospinal neurons after spinal cord injury. *J. Neurosci.* **29**: 14932–14941. [Medline] [CrossRef]
39. Scheff, S. W., Rabchevsky, A. G., Fugaccia, I., Main, J. A. and Lumpp, J. E. Jr. 2003. Experimental modeling of spinal cord injury: characterization of a force-defined injury device. *J. Neurotrauma* **20**: 179–193. [Medline] [CrossRef]
40. Seo, M. S., Jeong, Y. H., Park, J. R., Park, S. B., Rho, K. H., Kim, H. S., Yu, K. R., Lee, S. H., Jung, J. W., Lee, Y. S. and Kang, K. S. 2009. Isolation and characterization of canine umbilical cord blood-derived mesenchymal stem cells. *J. Vet. Sci.* **10**: 181–187. [Medline] [CrossRef]
41. Shetty, P., Cooper, K. and Viswanathan, C. 2010. Comparison of proliferative and multilineage differentiation potentials of cord matrix, cord blood, and bone marrow mesenchymal stem cells. *Asian J. Transfus. Sci.* **4**: 14–24. [Medline] [CrossRef]
42. Shuman, S. L., Bresnahan, J. C. and Beattie, M. S. 1997. Apoptosis of microglia and oligodendrocytes after spinal cord contusion in rats. *J. Neurosci. Res.* **50**: 798–808. [Medline] [CrossRef]
43. Siegenthaler, M. M., Tu, M. K. and Keirstead, H. S. 2007. The extent of myelin pathology differs following contusion and transection spinal cord injury. *J. Neurotrauma* **24**: 1631–1646. [Medline] [CrossRef]
44. Silver, J. and Miller, J. H. 2004. Regeneration beyond the glial scar. *Nat. Rev. Neurosci.* **5**: 146–156. [Medline] [CrossRef]
45. Swanger, S. A., Neuhuber, B., Himes, B. T., Bakshi, A. and Fischer, I. 2005. Analysis of allogeneic and syngeneic bone marrow stromal cell graft survival in the spinal cord. *Cell Transplant.* **14**: 775–786. [Medline] [CrossRef]
46. Sykova, E. and Jendelova, P. 2005. Magnetic resonance tracking of implanted adult and embryonic stem cells in injured brain and spinal cord. *Ann. N. Y. Acad. Sci.* **1049**: 146–160. [Medline] [CrossRef]
47. Taub, M., Wang, Y., Szczesny, T. M. and Kleinman, H. K. 1990. Epidermal growth factor or transforming growth factor alpha is required for kidney tubulogenesis in matrigel cultures in serum-free medium. *Proc. Natl. Acad. Sci. U.S.A.* **87**: 4002–4006. [Medline] [CrossRef]
48. Troyer, D. L. and Weiss, M. L. 2008. Wharton's jelly-derived cells are a primitive stromal cell population. *Stem Cells* **26**: 591–599. [Medline] [CrossRef]
49. Uemura, M., Refaat, M. M., Shinoyama, M., Hayashi, H., Hashimoto, N. and Takahashi, J. 2010. Matrigel supports survival and neuronal differentiation of grafted embryonic stem cell-derived neural precursor cells. *J. Neurosci. Res.* **88**: 542–551. [Medline]
50. Wagner, W., Wein, F., Seckinger, A., Frankhauser, M., Wirkner, U., Krause, U., Blake, J., Schwager, C., Eckstein, V., Ansorge, W. and Ho, A. D. 2005. Comparative characteristics of mesenchymal stem cells from human bone marrow, adipose tissue, and umbilical cord blood. *Exp. Hematol.* **33**: 1402–1416. [Medline] [CrossRef]
51. Webb, A. A., Jeffery, N. D., Olby, N. J. and Muir, G. D. 2004. Behavioural analysis of the efficacy of treatments for injuries to the spinal cord in animals. *Vet. Rec.* **155**: 225–230. [Medline] [CrossRef]
52. Yang, C. C., Shih, Y. H., Ko, M. H., Hsu, S. Y., Cheng, H. and Fu, Y. S. 2008. Transplantation of human umbilical mesenchymal stem cells from Wharton's jelly after complete transection of the rat spinal cord. *PLoS ONE* **3**: e3336. [Medline] [CrossRef]
53. Zai, L. J. and Wrathall, J. R. 2005. Cell proliferation and replacement following contusive spinal cord injury. *Glia* **50**: 247–257. [Medline] [CrossRef]
54. Zhang, H. T., Cheng, H. Y., Cai, Y. Q., Ma, X., Liu, W. P., Yan, Z. J., Jiang, X. D. and Xu, R. X. 2009. Comparison of adult neurospheres derived from different origins for treatment of rat spinal cord injury. *Neurosci. Lett.* **458**: 116–121. [Medline] [CrossRef]